(1985); J. M. Thomas *et al.*, *J. Ind. Microbiol.* **4**, 109 (1989).
5. J. J. Cooney, in *Petroleum Microbiology*, R. M. Atlas, Ed. (Macmillan, New York, 1984), pp. 399–433; G. Floodgate, in *ibid.*, pp. 355–397; D. M. Karl, in *Bacteria in Nature*, J. S. Poindexter and E. R. Leadbetter, Eds. (Plenum, New York, 1986), pp. 85–176.
6. J. C. Spain *et al.*, *Appl. Environ. Microbiol.* **48**, 944 (1984); R. L. Raymond, J. O. Hudson, V. W. Jamison, *Appl. Environ. Microbiol.* **31**, 522 (1976).
7. The field study by L. Semprini *et al.* [*Ground Water* **28**, 715 (1990)] is exceptional. Its success can be attributed to field instrumentation, a shallow confined aquifer, and the simultaneous metabolism of oxygen, methane, and chlorinated ethenes.
8. R. C. Borden and P. B. Bedient, *Water Res. Bull.* **23**, 629 (1987); C. Y. Chiang *et al.*, *Ground Water* **27**, 823 (1989).
9. P. V. Cline and D. R. Viste, *Waste Manage. Res.* **3**, 351 (1985); F. H. Chapelle and D. R. Lovley, *Appl. Environ. Microbiol.* **56**, 1865 (1990).
10. T. W. Federle and G. M. Pastwa, *Ground Water* **26**, 761 (1988); H. F. Ridgeway *et al.*, *Appl. Environ. Microbiol.* **56**, 3565 (1990). Microbial counts do not necessarily reflect in situ metabolic activity.
11. G. M. Klecka *et al.*, *Ground Water* **28**, 534 (1990); W. C. Ghiorse and J. T. Wilson. *Adv. Appl. Microbiol.* **33**, 107 (1988). Laboratory data describing biodegradation of various organic chemicals [M. Alexander, *Science* **211**, 132 (1981); W. C. Evans, *Nature* **270**, 17 (1977); J. F. Quensen, J. M.Tiedje, S. A. Boyd, *Science* **242**, 752 (1988); S. Dagley, *Surv. Prog. Chem.* **8**, 121 (1977)] show that microorganisms in soil and water have the potential to catalyze chemical reactions. However, microbial activity in disturbed environmental samples contained by laboratory vessels cannot be equated to in situ activity (*5*).
12. Coal tar is a black material produced from coal gasification processes [J. F. Villaume, in *Hazardous and Toxic Wastes: Technology Management and Health Effects*, S. K. Majumdar and E. W. Miller, Eds. (Pennsylvania Academy of Science, Easton, PA, 1984), pp. 362–375]. A single truckload of coal tar was buried in a forested area in the northeastern United States. This site has been characterized under EPRI research projects 2879-1 and 2879-12 [B. B. Taylor *et al.*, in *Proceedings: Environmental Research Conference on Groundwater Quality and Waste Disposal* (Electric Power Research Institute, EN-6749, Palo Alto, CA), pp. 26-1–26-12]. Sediments were 80 to 99% sand. Subsamples of materials used in biodegradation assays were analyzed for PAHs by gas chromatography (GC) and GC/mass spectrometry by Cambridge Analytical Associates, Inc., Boston, MA, under EPRI contract 2879-1.
13. Aseptic coring procedures followed established principles (*2, 4, 16, 17*). Depths selected for analyses were 1 to 2 m (unsaturated zone), 2.3 to 3 m (water table interface), 4 to 5, and 5 to 6 m (shallow and deep saturated zones). Additional details appear in EPRI Final Report RP 2879-5.
14. PHB is an intermediary metabolite in lignin biodegradation [J. P. Martin and K. Haider, in *Lignin Biodegradation: Microbiology, Chemistry, and Potential Applications*, T. K. Kirk, T. Higuchi, H. Chang, Eds. (CRC Press, Boca Raton, FL, 1980), vol. 1, pp. 77–100] that is metabolized by many aerobic soil bacteria.
15. Conversion of organic compounds to inorganic compounds (mineralization) was measured by standard $^{14}CO_2$ trapping methods. Radiolabeled [1-^{14}C]naphthalene (80 mCi/mmol, >98% radiopurity), [9-^{14}C]phenanthrene (10.4 mCi/mmol, >99% radiopurity), and *p*-hydroxybenzoate (ring UL 7.7 mCi/mmol, >99% radiopurity) were purchased from Sigma Radiochemicals (St. Louis, MO). Compounds were dissolved, filter-sterilized (naphthalene and phenanthrene in acetone before eing diluted 100-fold in distilled water, *p*-hydroxybenzoate in distilled water) and then added to sterile 125-ml flasks containing 4 g of aseptically distributed sediment sample. Each flask received 0.04 μCi of ^{14}C-labeled and unlabeled naphthalene, phenanthrene, or *p*-hydroxybenzoate at concentrations of 1 ppm. An abiotic control flask was prepared in each test by autoclaving the sample for 1 hour and adding 1 ml of 1 M $HgCl_2$ before addition of carbon compounds. The flasks were sealed with lids suspending a small plastic cup (containing 0.6 ml of CO_2 trapping agent) and incubated statically at 23°C. At each sampling time, trapping agent was withdrawn, counted in a scintillation counter, then replenished.
16. D. L. Balkwill and W. C. Ghiorse, *Appl. Environ. Microbiol.* **50**, 580 (1985); J. T. Wilson *et al.*, *Ground Water* **21**, 134 (1983).
17. J. L. Sinclair and W. C. Ghiorse, *Geomicrobiol. J.* 7, 15 (1989); *Appl. Environ. Microbiol.* **53**, 1157 (1987).
18. T. D. Brock and M. T. Madigan, *Biology of Microorganisms* (Prentice-Hall, Englewood Cliffs, NJ, ed. 5, 1988). Lag periods occur when enzyme synthesis or population growth precede biodegradation; their absence indicates a state of metabolic readiness.
19. Total counts normally exceed viable counts by 2 to 3 orders of magnitude [D. B. Roszak and R. R. Colwell, *Microbiol. Rev.* **51**, 365 (1987); (*16, 17*)].
20. T. Fenchel, *Ecology of Protozoa* (Science Tech, Madison, WI, 1987); W. Foissner, *Prog. Protistol.* **2**, 69 (1987); J. D. Stout, *Adv. Microbiol. Ecol.* **4**, 1 (1980).
21. J. L. Sinclair, in *Proceedings of the First International Symposium on Microbiology of the Deep Subsurface*, C. B. Fliermans and T. C. Hazen, Eds. (WSRC Information Services, Aiken, SC, 1991), pp. 3-35–3-45.
22. S. N. Levine and W. C. Ghiorse, in *ibid*, pp. 5-31–5-45; J. K. Fredrickson *et al.*, *Geomicrobiol. J.* 7, 53 (1989).
23. Adaptational biodegradation is indicated by an acceleration in microbiological destruction of chemicals after their introduction into a given environment (*3, 4*). Adaptation has been reported in subsurface microbial communities to PAHs (*4*) and in other settings (*3*).
24. R. Kolwitz and M. Marsson, *Int. Rev. Hydrobiol. Hydrogr.* **2**, 126 (1909) [cited in Fenchel (*20*)].
25. H. T. Tribe, *Soil Sci.* **92**, 61 (1961); C. R. Curds, *Annu. Rev. Microbiol.* **36**, 27 (1982).
26. E. Hartwig, *Senckenbergiana Marit.* **16**, 121 (1984) [cited in Foissner (*20*)].
27. J. R. Vestal *et al.*, in *Petroleum Microbiology*, R. M. Atlas, Ed. (Macmillan, New York, 1984), pp. 475–505.
28. A. Rogerson and J. Berger, *J. Gen. Appl. Microbiol.* **29**, 41 (1983).
29. We thank B. B. Taylor and J. A. Ripp for collaborative field assistance and analytical data that were obtained under EPRI contract 2879-1. This investigation was carried out under EPRI project RP 2879-5. Technical assistance from L. Anguish, S. Best, C. Thomas, and A. Winding is gratefully acknowledged.

13 November 1990; accepted 13 March 1991

Control of *doublesex* Alternative Splicing by *transformer* and *transformer-2* in *Drosophila*

KAZUYUKI HOSHIJIMA, KUNIO INOUE, IKUKO HIGUCHI, HIROSHI SAKAMOTO, YOSHIRO SHIMURA*

Sex-specific alternative processing of *doublesex* (*dsx*) precursor messenger RNA (pre-mRNA) regulates somatic sexual differentiation in *Drosophila melanogaster*. Cotransfection analyses in which the *dsx* gene and the female-specific *transformer* (*tra*) and *transformer-2* (*tra-2*) complementary DNAs were expressed in *Drosophila* Kc cells revealed that female-specific splicing of the *dsx* transcript was positively regulated by the products of the *tra* and *tra-2* genes. Furthermore, analyses of mutant constructs of *dsx* showed that a portion of the female-specific exon sequence was required for regulation of *dsx* pre–messenger RNA splicing.

SOMATIC SEXUAL DIFFERENTIATION IN *Drosophila melanogaster* is accomplished by a hierarchy of regulatory genes that act in response to the number of X chromosomes relative to the number of sets of autosomes in a cell (the X:A ratio) (*1*). One of these regulatory genes, *dsx*, is required for terminal sexual differentiation in both male and female flies (*2*). Molecular analyses have shown that the *dsx* transcript undergoes sex-specific RNA processing (splicing and cleavage-polyadenylation reactions), which leads to the production of two distinct sex-specific polypeptides (Fig. 1A) (*3*). The male- and female-specific *dsx* products regulate sexual differentiation by repressing the female- and male-specific terminal differentiation functions, respectively (*2*). Genetic analyses have shown that the *tra* and *tra-2* genes are required for regulation of sex-specific *dsx* expression (*4*). In males, *tra* produces a nonfunctional product, whereas the female-specific *tra* product is functional and is produced by alternative splicing of *tra* pre-mRNA (*5, 6*). The *tra-2* product is also required for proper differentiation of male germ line cells (*7*). The predicted polypeptide encoded by *tra-2* (*8*) contains a domain of 90 amino acids that is also found in RNA binding proteins (*9*). In addition, the predicted protein sequences encoded by *tra-2* (*8*) and *tra* (*10*) contain arginine- and serine-rich regions that are characteristic of proteins that participate in RNA processing (*9*). Although these findings suggest that the products of *tra* and *tra-2* function in the regulation of alternative processing of *dsx* pre-mRNA, direct evidence has been lacking.

To decipher the mechanism of alternative processing of *dsx*, we constructed a plasmid

Department of Biophysics, Faculty of Science, Kyoto University, Kyoto 606, Japan.

*To whom correspondence should be addressed.

(copia-dsx) that contained the portion of *dsx* that extends from the third exon (found in both male- and female-specific transcripts) to the male-specific fifth exon, under the control of the copia element long terminal repeat (LTR) (*6*); in this construct, a portion of the intron between the female-specific fourth exon and the male-specific fifth exon was deleted (*11*). When copia-dsx was transfected into Kc cells, the male-specific mRNA was generated almost exclusively (Fig. 1B, lanes 1 and 5). To determine whether the *tra* and *tra-2* products affected *dsx* pre-mRNA processing, we transfected copia-dsx with the female-specific *tra* cDNA (*12*), the *tra-2* cDNA (*8*), or both, under the control of the *Drosophila* heat shock protein 70 gene (*hsp70*) promoter (*6*) (hsp-tra and hsp-tra-2, respectively). When copia-dsx was cotransfected with either hsp-tra or hsp-tra-2, the male-specific *dsx* mRNA was generated along with a considerable amount of female-specific mRNA (Fig. 1B, lanes 2, 3, 6, and 7). In contrast, only the female-specific *dsx* mRNA was produced when copia-dsx was cotransfected with both hsp-tra and hsp-tra-2 (Fig. 1B, lanes 4 and 8). Therefore, both the female-specific *tra* product and the *tra-2* product are necessary for maximal production of female-specific *dsx* mRNA. This finding is consistent with results obtained with mutant flies (*4*). Because we could not detect any *dsx* RNAs in Kc cells not transfected with copia-dsx (*13*), the amount of endogenous *dsx* mRNAs seems to be very low in these cells. However, the fact that the small amount of endogenous *dsx* mRNA present in Kc cells is of the female type (*3*) implies that the female-specific *tra* product and the *tra-2* product are produced endogenously in these cells, which could explain why a small amount of female-specific *dsx* mRNA was detected when copia-dsx alone was transfected into Kc cells and why cotransfection of copia-dsx with either hsp-tra or hsp-tra-2 resulted in submaximal production of female-specific *dsx* mRNA (Fig. 1B, lanes 1 to 3).

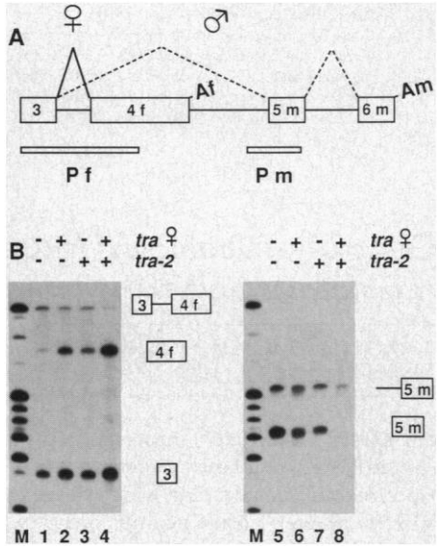

Fig. 1. Effect of *tra* and *tra-2* cDNA products on the splicing patterns of *dsx* pre-mRNA in Kc cells. (**A**) Sex-specific processing of *dsx* pre-mRNA. Boxes and the lines between boxes represent the exon and intron sequences, respectively. In female flies, the third exon is spliced to the fourth exon (indicated by solid line) and the female polyadenylation site (Af) is used. In male flies, the third exon is spliced to the fifth exon (indicated by dashed line) and the male polyadenylation site (Am) is used. Two types of RNA probe used in the ribonuclease (RNase) protection assay are shown below (Pf and Pm). (**B**) Cotransfection analyses of copia-dsx with hsp-tra and hsp-tra-2 in Kc cells. A *dsx* genomic fragment that contains the third exon to the fifth exon (*11*) was fused downstream of the copia LTR (*6*). The female-specific *tra* cDNA (*5*) and the *tra-2* cDNA (*8*) were individually fused to the promoter of the *hsp70* gene (*6*). A copia-dsx plasmid was transfected into Kc cells without or with the *tra-2* cDNA or the female-specific *tra* cDNA as shown. RNA products were analyzed by RNase protection (*6*) with Pf (lanes 1 to 4) or Pm (lanes 5 to 8) as the probes. The structures of the RNA molecules are illustrated at the right. M, Hpa II digest of pBR used as a source of molecular size markers. The RNA band designated 4f represents the female-specific splicing product of *dsx* pre-mRNA.

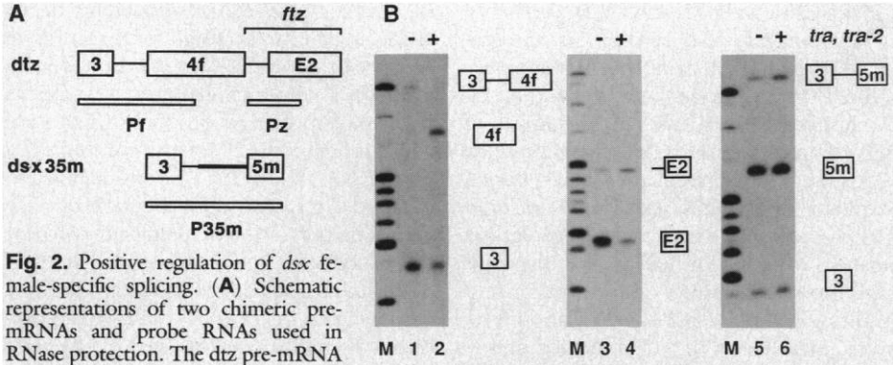

Fig. 2. Positive regulation of *dsx* female-specific splicing. (**A**) Schematic representations of two chimeric pre-mRNAs and probe RNAs used in RNase protection. The dtz pre-mRNA contains the region of *dsx* from the third exon to the fourth exon, followed by a portion of the first intron and the second exon of *ftz* (*15*); the polyadenylation signal of the *dsx* fourth exon was deleted. The dsx35m pre-mRNA contains the region of *dsx* from the third exon to the fifth exon but lacks the 3′ half of the third intron, including the female-specific acceptor region, and the fourth exon (*16*). (**B**) Expression of dtz and dsx35m pre-mRNAs in the absence or presence of the female-specific *tra* cDNA and *tra-2* cDNA in Kc cells as shown. The dtz (lanes 1 to 4) and dsx35m (lanes 5 and 6) pre-mRNAs were expressed under the control of the copia LTR. RNA products were analyzed by RNase protection with the Pf (lanes 1 and 2), Pz (lanes 3 and 4), and P35m (lanes 5 and 6) probes shown in (A). M, Hpa II digest of pBR. In the case of dtz pre-mRNA, the RNA band designated 4f represents the female-specific splicing product. The RNA band E2 represents the product of splicing between exons 3 and E2. In the case of dsx35m pre-mRNA, the RNA band 5m represents the product of splicing between exons 3 and 5m.

The increase in female-specific *dsx* mRNA seen after coexpression of *dsx* with *tra* and *tra-2* could occur by several different mechanisms: (i) activation of the female-specific acceptor site immediately upstream of the fourth exon; (ii) activation of the cleavage-polyadenylation reaction at the site immediately downstream of the female exon; (iii) inhibition of the male-specific acceptor site immediately upstream of the male-specific fifth exon; or (iv) a combination of these mechanisms. These possible mechanisms were previously discussed by Nagoshi and Baker (*14*), who also suggested that activation of the female-specific acceptor site was the most plausible mechanism. To determine which of the above mechanisms is operative, we constructed two chimeric plasmids (Fig. 2A): copia-dtz (*15*) contains the region of *dsx* that extends from the common third exon to the female-specific fourth exon, followed by part of the intron and the second exon of *fushitarazu* (*ftz*); copia-dsx35m (*16*) contains the region of *dsx* that extends from the common third exon to the male-specific fifth exon, but lacks the entire female-specific exon and portions of its adjacent introns.

When copia-dtz was transfected into Kc cells, we observed almost exclusively the product of splicing between the *dsx* common exon and the *ftz* exon, with a small amount of the female-specific product of splicing between the third common exon and the female-specific fourth exon (Fig. 2B, lanes 1 and 3). In contrast, when copia-dtz was cotransfected with both hsp-tra and hsp-tra-2, the female-specific splicing product was generated, and the splicing product that contains the *ftz* exon decreased concomitantly (Fig. 2B, lanes 2 and 4). Because copia-dtz does not contain either the polyadenylation site (Fig. 1, Af) immediately downstream of the female-specific exon or the male-specific acceptor site, we could exclude the possibilities that the female-

specific splicing product is generated by activation of the cleavage-polyadenylation reaction or by inhibition of the male-specific acceptor site. Our results are compatible only with the remaining possibility, that the female-specific acceptor site immediately upstream of the fourth exon is activated. The results obtained with copia-dsx35m also support this notion. In this case, the product of splicing between the common and the male-specific exons was observed in the absence or presence of hsp-tra and hsp-tra-2 (Fig. 2B, lanes 5 and 6). Thus, we conclude that the increase in female-specific *dsx* mRNA seen after coexpression of female-specific *tra* and *tra-2* products results from activation of the female-specific acceptor site.

The results with copia-dtz (Fig. 2B) indicate that most of the information for the regulation of *dsx* alternative splicing lies within the region that spans from the third common exon up to and including the female-specific exon. These results are consistent with analyses of mutations that disrupt *dsx* alternative splicing (*14*). The female-specific exon contains six copies of a tandemly interspersed 13-nucleotide (nt) sequence, TC(T/A)(T/A)CAATCAACA (*3, 14*). To examine whether the repetitive 13-nt sequences are responsible for regulation of *dsx* splicing, we analyzed deletion and insertion mutants of copia-dsx (*17*) by cotransfection (Fig. 3). When three copies of the 13-nt sequence were deleted (R1·5·6), high efficiency female-specific splicing was still observed in the presence of *tra* and *tra-2*. However, removal of the remaining 13-nt sequences (R5·6, R6, R1, R0) caused a proportional reduction in the amount of female-specific splicing product and an increase in the amount of the male-specific splicing product. Introduction of the 13-nt sequences in the sense orientation (SR) into the mutant that had all the 13-nt repeats deleted (R0) restored female-specific splicing, whereas introduction in the antisense orientation (ASR) did not. These results indicate that the 13-nt sequences are responsible for activation of female-specific splicing.

It has been suggested that the female-specific acceptor sequence of *dsx* is suboptimal for splicing—because the polypyrimidine stretch, one of the essential splicing signals (*18*), is interrupted by purine residues—and that this suboptimal signal is important for regulation of *dsx* splicing (*3, 14*). The male-specific acceptor site of *dsx*, the sequence of which matches more closely the consensus sequence for *Drosophila* splice acceptor sites (*3*), is almost exclusively used in male flies. To examine the importance of the polypyrimidine stretch in the female acceptor sequence, we introduced substitutions into copia-dtz that increased the length of the polypyrimidine stretch. When one of the mutant plasmids, copia-dtz(Py18), in which five nucleotide substitutions give rise to 18 consecutive pyrimidines (*19*), was transfected into Kc cells, female-specific splicing occurred efficiently irrespective of the presence of the *tra* or *tra-2* products, whereas splicing occurred only in the presence of the *tra* and *tra-2* products with copia-dtz (Fig. 4). The same result was obtained with copia-dtz(Py13) (Fig. 4A) and with derivatives of copia-dtz(Py18) and copia-dtz(Py13) plasmids in which the 13-nt sequences in the female exon had been deleted (*20*). The results with these mutations suggest that the female-specific acceptor site has a suboptimal polypyrimidine stretch, which could explain why the female-specific acceptor site is not used in male flies.

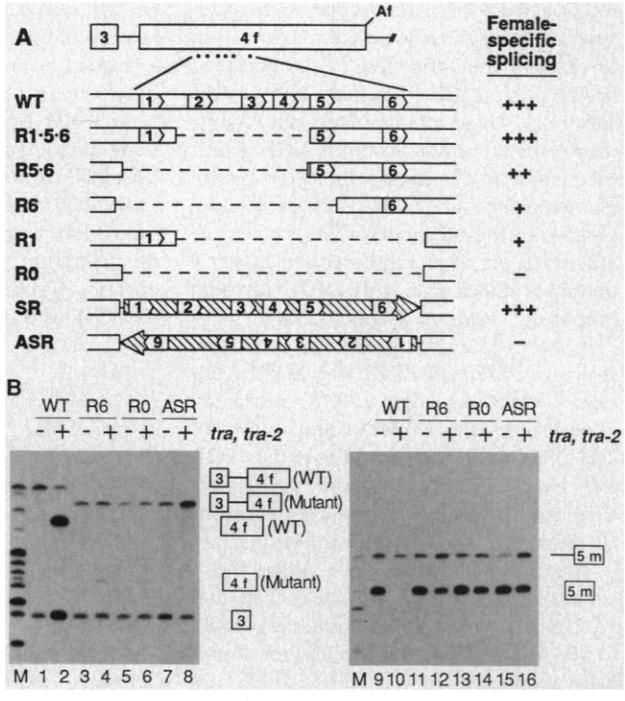

Fig. 3. Regulatory element of *dsx* female-specific splicing. (**A**) Six repeats of a 13-nt sequence, TC(T/A)(T/A)CAATCAACA, are present in the female-specific fourth exon of *dsx* (*3*), as shown in the top line (dots). Mutant constructs were expressed with the female-specific *tra* cDNA and the *tra-2* cDNA in Kc cells. The structures of the wild-type (WT) and mutant constructs are shown (*17*). Some or all of the six repeats were deleted (R1·5·6, R5·6, R6, R1, R0). A PCR (polymerase chain reaction) fragment (*17*) that contains the six repeats was inserted into the R0 construct in the correct (SR) or the opposite (ASR) orientation. Numbered pentagons, 13-nt sequences; dashed lines, deleted regions; hatched arrows, PCR fragments that contain the six repeats. The relative efficiency of female-specific splicing was calculated as the ratio of the amount of female-specific product to that of the third common exon and expressed as a percentage of the value for the wild-type construct: 100 to 85% (+++), 85 to 65% (++), 65 to 30% (+), and 0% (−). (**B**) Transfection analyses with some of the constructs described in (A). Each plasmid shown at the top of the lanes was transfected with (+) or without (−) hsp-tra and hsp-tra-2. RNA products were analyzed with Pf (lanes 1 to 8) or Pm (lanes 9 to 16) probes as described in Fig. 1. The structures of the RNA molecules are illustrated at the right. The length of protected fragments corresponding to pre-mRNA and the female-specific splicing product are different between the wild-type and mutant plasmids. M, Hpa II digest of pBr.

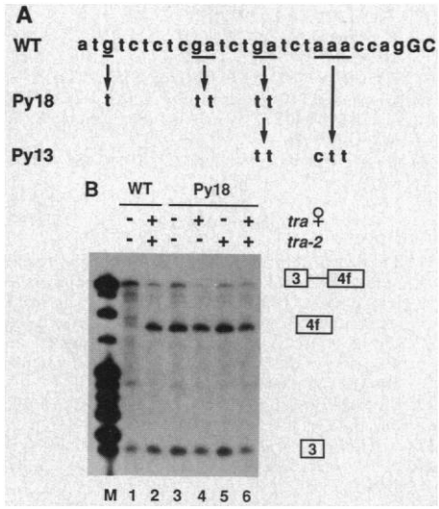

Fig. 4. Effect of base substitutions in the female-specific acceptor region on *dsx* pre-mRNA splicing. (**A**) Nucleotide sequences of the female-specific acceptor region of the wild-type and mutant copia-dtz plasmids. Small and capital letters represent nucleotide sequences of the intron and the following fourth exon, respectively. Mutant copia-dtz plasmids, copia-dtz(Py18) and copia-dtz(Py13), contain five purine-to-pyrimidine substitutions; these substitutions produced 18 and 13 consecutive pyrimidines, respectively. (**B**) Transfection of copia-dtz(Py18) in Kc cells. Copia-dtz(Py18) and copia-dtz were expressed without or with the *tra-2* cDNA or the female-specific *tra* cDNA as shown. RNA products obtained with the mutant plasmid were analyzed by RNase protection with Pf(Py18) as the probe, which corresponds to the dtz(Py18) sequence. whereas RNA products with the WT construct were analyzed with the same Pf probe as in Fig. 1. M, Hpa II digest of pBR.

Our results show that the presence of the female-specific *tra* and the *tra-2* products promote female-specific splicing of *dsx* pre-mRNA and that the 13-nt sequences in the female exon and the female-specific acceptor sequence participate in regulation of *dsx* expression. The *tra* and *tra-2* products may interact directly with the 13-nt sequences in the female-specific exon, and such interactions may allow the suboptimal female-specific polypyrimidine stretch to be recognized as a splicing signal, thus resulting in enhancement of the use of the female-specific acceptor site.

REFERENCES AND NOTES

1. R. Nothiger and M. Steinmann-Zwicky, *Trends Genet.* **1**, 209 (1985); T. W. Cline, in *Origin and Evolution of Sex*, H. O. Halvorson and A. Monroy, Eds. (Liss, New York, 1985), pp. 301–327; B. S. Baker, *Nature* **340**, 521 (1989).
2. B. S. Baker and K. A. Ridge, *Genetics* **94**, 383 (1980).
3. B. S. Baker and M. F. Wolfner, *Genes Dev.* **2**, 477 (1988); K. C. Burtis and B. S. Baker, *Cell* **56**, 997 (1989).
4. R. N. Nagoshi, M. McKeown, K. C. Burtis, J. M. Belote, B. S. Baker, *Cell* **53**, 229 (1988).
5. M. McKeown, J. M. Belote, R. T. Boggs, *ibid.*, p. 887; B. A. Sosnowski, J. M. Belote, M. McKeown, *ibid.* **58**, 449 (1989).
6. K. Inoue, K. Hoshijima, H. Sakamoto, Y. Shimura, *Nature* **344**, 461 (1990).
7. T. Schupbach, *Dev. Biol.* **89**, 117 (1982); J. M. Belote and B. S. Baker, *Proc. Natl. Acad. Sci. U.S.A.* **79**, 1568 (1982); *Dev. Biol.* **95**, 512 (1983).
8. H. Amrein, M. Gorman, R. Nothiger, *Cell* **55**, 1025 (1988); T. J. Goralski, J.-E. Edstrom, B. S. Baker, *ibid.* **56**, 1011 (1989).
9. C. C. Query, R. C. Bentley, J. D. Keene, *ibid.* **57**, 89 (1989); I. W. Mattaj, *ibid.*, p. 1.
10. J. M. Belote, M. McKeown, R. T. Boggs, R. Ohkawa, B. A. Sosnowski, *Dev. Genet.* **10**, 143 (1989).
11. The region from and including the entire third exon to the Pvu II site located 1284 bp downstream of the female acceptor site, and the region from the Acc I site located 250 bp upstream of the male acceptor site to the site located 64 bp downstream of the donor site of the fifth exon, were joined and inserted into the copia vector.
12. M. McKeown, J. M. Belote, R. T. Boggs, *Cell* **53**, 887 (1988).
13. K. Hoshijima *et al.*, unpublished observations.
14. R. N. Nagoshi and B. S. Baker, *Genes Dev.* **4**, 89 (1990).
15. The *dsx* fragment that extends from the third exon to 1128 bp downstream of the female acceptor site and which excludes the polyadenylation signal (Af) was fused to the *ftz* fragment that contains a portion of the intron and the following second exon {corresponding to bases 825 to 2534 of the published sequence [A. Laughon and M. P. Scott, *Nature* **310**, 25 (1984)]}. The resulting fragment was inserted into the copia vector.
16. The region from the third exon (138 bp) to the site 48 bp downstream of the donor site of the third exon, and the region from the site 250 bp upstream of the male acceptor site to the site 64 bp downstream of the donor site of the fifth exon, were joined and inserted into the copia vector.
17. The copia-dsx deletion mutants were constructed as follows: the regions between 345 to 460 bp (R1·5·6), 234 to 459 bp (R5·6), 190 to 480 bp (R6), 344 to 599 bp (R1), or 234 to 599 bp (R0) downstream of the female acceptor site were deleted from copia-dsx, and Kpn I linkers were inserted. A polymerase chain reaction (PCR) fragment that contained the region 268 to 627 bp downstream of the female-specific acceptor site was inserted at the Kpn I linker of the R0 construct in the correct orientation (SR) or in the opposite orientation (ASR). PCR was performed essentially as described [R. K. Saiki *et al.*, *Science* **239**, 487 (1988)].
18. M. R. Green, *Annu. Rev. Genet.* **20**, 671 (1986).
19. Oligonucleotide-directed mutagenesis was performed essentially as described [M. J. Zoller and M. Smith, *Methods Enzymol.* **100**, 468 (1983)].
20. The region 340 to 1128 bp downstream of the female acceptor site was deleted from copia-dtz, copia-dtz(Py18), and copia-dtz(Py13). Pre-mRNA expressed from the deletion construct of copia-dtz was spliced at the *ftz* acceptor site even in the presence of the *tra* and *tra-2* products in Kc cells.

21. We thank M. McKeown for *tra* cDNA and H. Amrein for *tra-2* cDNA. Supported by Grant-in-Aid 62065009 for specially promoted research from the Ministry of Education, Science and Culture of Japan.

1 November 1990; accepted 1 March 1991

Solution Structure of FKBP, a Rotamase Enzyme and Receptor for FK506 and Rapamycin

STEPHEN W. MICHNICK, MICHAEL K. ROSEN, THOMAS J. WANDLESS, MARTIN KARPLUS,* STUART L. SCHREIBER*

Immunophilins, when complexed to immunosuppressive ligands, appear to inhibit signal transduction pathways that result in exocytosis and transcription. The solution structure of one of these, the human FK506 and rapamycin binding protein (FKBP), has been determined by nuclear magnetic resonance (NMR). FKBP has a previously unobserved antiparallel β-sheet folding topology that results in a novel loop crossing and produces a large cavity lined by a conserved array of aromatic residues; this cavity serves as the rotamase active site and drug-binding pocket. There are other significant structural features (such as a protruding positively charged loop and an apparently flexible loop) that may be involved in the biological activity of FKBP.

FKBP IS A SOLUBLE, CYTOSOLIC RE-ceptor (*1, 2*) for the immunosuppressants FK506 and rapamycin (*3*). Both FKBP and cyclophilin (*4–6*), which is a receptor for the immunosuppressant cyclosporin A (CsA), catalyze the interconversion of cis- and trans-rotamers of the peptidyl-prolyl amide bond of peptide and protein substrates. These rotamases are inhibited by their respective immunosuppressive ligands. Mechanistic studies suggest that a complex of immunophilin (immunosuppressant binding protein) and ligand interferes with the intracellular transport of proteins involved in signal transduction pathways associated with both exocytosis (7) and transcription (*3, 8*).

In this report we present the solution structure of human FKBP obtained by nuclear Overhauser effect (NOE)–restrained molecular dynamics (rMD) simulations (*9*). The NMR structures satisfying the NOE and empirical energy function restraints have backbone root-mean-square deviations (RMSDs) from the refined average structure in the range of 0.80 to 1.4 Å for the β strands, 0.19 to 0.40 Å for the α helix, and 1.02 Å to 1.72 Å for all residues except 83 to 90 (see below). Many side chains, particularly aromatics, are well defined. FKBP has a novel folding topology in that two loops that connect the strands of an antiparallel β sheet cross one another. Hydrophobic side chains in the core of the protein form a large, deep pocket that includes the rotamase active site and the drug-binding site. The structure of the binding site appears to be highly conserved in related FK506- and rapamycin-binding proteins.

Sequence-specific assignments of 92% of the observable ^1H resonances in FKBP have been made by use of a combination of homonuclear and heteronuclear two-dimensional NMR techniques as reported earlier (*10*). Structural restraints for the dynamics simulations were obtained through empirical calibration of cross-peak magnitudes in nuclear Overhauser effect spectroscopy (NOESY) spectra recorded with mixing times

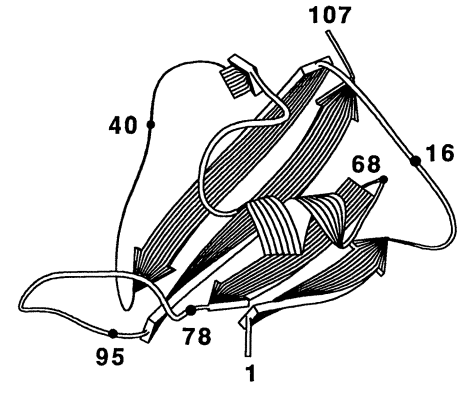

Fig. 1. α-Carbon ribbon drawing of human FKBP; the five-stranded β sheet, α helix, and connecting loops are indicated, as well as the COOH- and NH_2-termini and certain residues of interest.

Department of Chemistry, Harvard University, Cambridge, MA 02138.

*To whom correspondence should be addressed.